Proceedings of the Fifteenth International Conference on
Computational Structures Technology
Edited by: P. Iványi, J. Kruis and B.H.V. Topping
Civil-Comp Conferences, Volume 9, Paper 7.5
Civil-Comp Press, Edinburgh, United Kingdom, 2024
ISSN: 2753-3239, doi: 10.4203/ccc.9.7.5

Numerical and Experimental Tests of Steel-Concrete Composite Beam with an Innovative Connector Made of Corrugated Metal Sheet and Shot Nails

A. Derlatka, P. Lacki and P. Kania

Faculty of Civil Engineering, Czestochowa University of Technology, Czestochowa, Poland

Abstract

This article presents the possibility of applying innovative fasteners made of corrugated metal sheet in the dovetail-shape and shot nails to make a steel-concrete composite beam. The beam was built using fasteners made of metal sheet with a thickness of 1.00 mm and 2 or 4 shot nails into single sheet fold. The nails were shot through the sheet into the flange of the steel I-section. The 7.5 m long beam was subjected to a bending test. Based on the experimental studies, a numerical model of the beam was developed in the ADINA System program. The used concrete material model, taking into account the post-cracking and crushing behaviour allowed to locate critical areas of failure. The beam connectors showed sufficient load-bearing capacity and the concrete slab was the weakest component of the composite beam. The beam was damaged as a result of cracking in the slab and, as a consequence, local detachments of the corrugated sheet from the concrete slab. The proposed solution can be used as the fastener for steel-concrete composite structures ceilings of small utility public buildings.

Keywords: steel-concrete composite beam, connector, finite element analysis, ADINA, beam finite element simulation, static load.

1 Introduction

When a new type of fastener is developed, testing is required. One way is numerical calculations. Numerical simulations are widely used in steel-concrete composite structures under static [1–3] and dynamic loads [4]. In order to obtain reliable results,

numerical models must adequately represent the components of composite structures [5–7]. Therefore, appropriate types of finite elements should be assumed. Since the behaviour of composite beams exhibits significant non-linear effects, it is essential to properly model the interactions between the finite elements in such a way as to reflect the interactions between the components, especially steel beam and slab, steel beam and fasteners, and slab and fasteners.

In paper [8], the load capacity of an innovative connector for steel-concrete composite structures made of corrugated sheet in the shape of a dovetail and driven nails was analysed. The nails were driven through the lower fold of the sheet into the flange of the steel I-beam. The results of the push-out tests proved that the shape of the proposed sheet positively affects the connection of the reinforced concrete slab with the steel I-beam. At the same time, all fasteners analysed in [8], made of metal sheet with a thickness of 1.00 and 1.25 mm and of 2 and 4 nails in the corrugation of the sheet, were considered ductile in accordance with the requirements of Eurocode 4 [9].

This article presents the possibility of applying innovative fasteners made of corrugated sheet in the dovetail-shape and shot nails to make a steel-concrete composite beam. The 7.5 m long beam was subjected to a bending test. The metal sheet with a thickness of 1.00 mm was used to provide stay-in-place formwork for the monolithic slab. The beam was built using fasteners made of 2 nails in the span zone and 4 nails in the support zone. On the basis of the test results, the load capacity of the beam and its failure mode were determined, which made it possible to assess the possibility of using the beam with innovative connectors for the construction of lightweight ceilings in small public buildings. Based on the experimental studies carried out, a numerical model was developed in the ADINA System [10] program, reflecting the behaviour of the analysed composite beam. A concrete material model, taking into account the post-cracking and crushing behaviour was used [11]. Determination of fracture patterns made it possible to locate critical areas of failure.

2 Experimental program

As shown in Figure 1, the beam was constructed from the IPE 200 I-beam made of S235 structural steel. The corrugated sheets, galvanized on both sides, 1.00 mm thick, made of S280GD steel, were connected to the I-beam flange. The sheet was placed with the surface as after rolling, i.e. the surface of the sheet was not cleaned of grease so as not to improve the adhesion conditions. However, it should be remembered that the corrugated sheet has ribs on the upper folds, which affect the adhesion of concrete to this part of the sheet. The sheet was fixed to the I-beam with shot nails. The length of the beam was 7500 mm, while its width (corresponding to the width of the slab) was 1800 mm.

The nails were placed in two rows. The spacing of rows was 56.0 mm. In the support zones, i.e. along the length of 1510 mm, 4 nails were used per sheet fold. On the other hand, in the span zone, i.e. with the length of 4480 mm, only 2 nails were used per fold of the sheet.

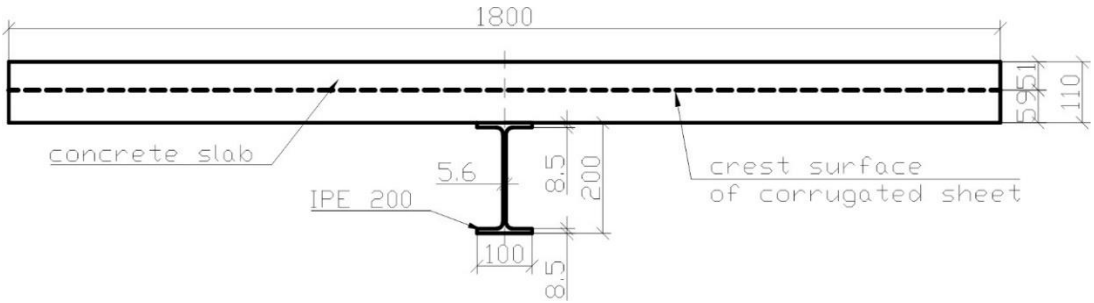

Figure 1: Cross-section of analysed steel-concrete composite beam.

The corrugated sheet, in addition to the connector function, also provided permanent formwork for the monolithic reinforced concrete slab. The reinforced concrete slabs were made of C20/25 class concrete. The thickness of the slab (above the folds of the sheet) was 51 mm, so that the total thickness of the plate was 110 mm. The width of the panels was 1800 mm so as to cover the entire width of the profiled sheet.

The reinforcement mesh was prepared from ϕ8 mm bars made of steel with a characteristic yield strength f_{sk} = 500 MPa and C ductility class according to PN-EN 1992-1-1 [12]. The transverse reinforcement was arranged according to the spacing of the sheet folds, i.e. every 140 mm. The longitudinal reinforcement bars are spaced every 125 mm. The beam was concreted under fully supported conditions. The beam was matured in an air environment. Bending tests were carried out 28 days after the beam was made.

To ensure the static scheme of the analysed beam as a free supported beam, the reinforced concrete slab was support on two steel U 200 profiles. The upper surface of the slab was loaded with 4 pneumatic actuators in the shape of cylinders with a diameter of 200 mm. On the lower surface of the corrugated sheet and the lower surface of the I-beam, 9 dial gauges were used to measure displacements. The spacing of actuators and sensors is shown in Figure 2.

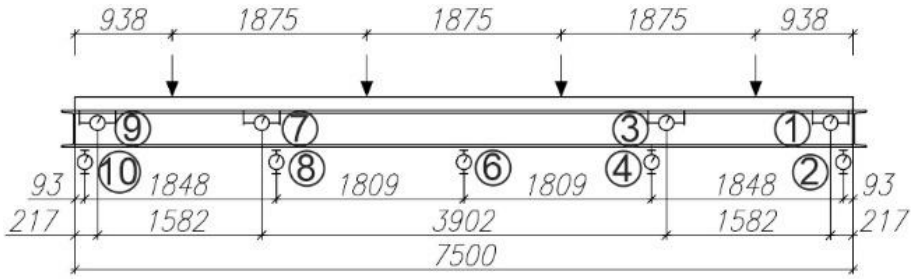

Figure 2: Scheme of arrangement of cylinders and dial gauges on beam.

3 Numerical model of composite beam

A numerical model was developed reflecting the behaviour of the analysed composite beam. Thanks to the numerical analysis, not only the displacement-load diagrams obtained in experimental studies were determined, but also detailed distributions of stresses and strains in individual components of the beam. In the numerical model of

the floor beam, the finite element method was used to describe the influence of mechanical loads on deformations and stresses. Numerical calculations were performed using the ADINA System program [10].

A schematic diagram of the numerical model of the composite beam with marked boundary conditions is shown in Figure 3. The red, pink, orange, green and purple colours represent the concrete slab, reinforcement bars, corrugated plate, steel beam and supports, respectively. The boundary conditions reflect a simply supported composite beam. Along the bottom edge of one support, all degrees of freedom are blocked (symbol B). On the other hand, along the lower edge of the second support, the degrees of freedom along the X axis (symbol C) were released. The load was applied to four actuators and is marked with blue arrows. The spacing of the actuators was assumed to be the same as the spacing on the experimental test stand.

In the ADINIA System program, the type of analysis depends, among others, on the material models, contact conditions and the type of applied load. In the numerical model of the composite steel-concrete beam, a non-linear analysis was used, taking into account large displacements and strains resulting from the adopted material models and the values of the assumed load.

The properties of the materials used in the numerical simulations are presented in Table 1 and Table 2. Material models were developed on the basis of data determined in experimental studies presented in this work and in [8]. Data not determined experimentally were assumed on the basis of EN 1992-1-1 and EN 1993-1-1 [12],[13]. Steel components (I-beam, sheets, nails, reinforcing bars) were described in the bilinear elastic-plastic model (von Mises yield criterion). An advanced concrete model available in the ADINA System program was used to simulate concrete assessing the possibility of concrete cracking. The uniaxial stress-strain relationship was the basis for the derivation of the multiaxial stress-strain relationship.

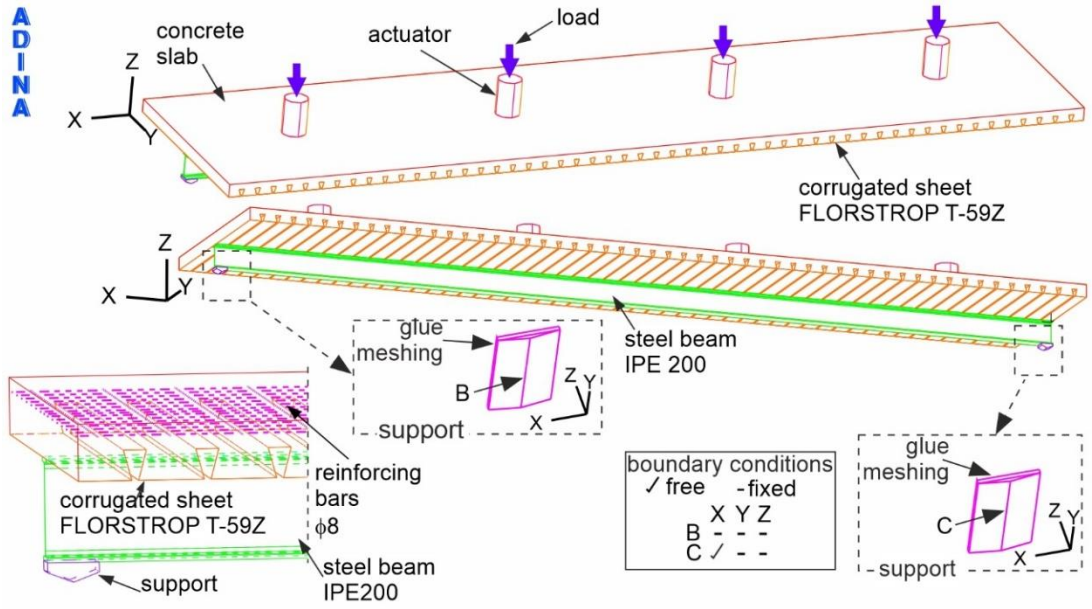

Figure 3: Numerical model of a composite beam.

Property	Material			
	Steel S235 (IPE 200)	Steel S280GD (1.00 mm thick)	Reinforcement steel fsk=500 MPa	Steel nails
Young's modulus E, GPa	210	210	205	193
Yield strength fy, MPa	339	300	500	950
Ultimate tensile strength fu, MPa	468	379	600	2180
Poisson's ratio ν	0.3	0.3	0.3	0.3
Density, kg/m3	7850	7850	7850	8000
Minimum elongation A5, %	26	18	16	5

Table 1: Properties of the steel used in the numerical model of beam.

Property	Value
	Concrete C20/25
Tangent modulus at zero strain Ecm, GPa	30
Uniaxial cut-off tensile stress fctm, MPa	2.2
Uniaxial maximum compressive stress fcm, MPa	-30.3
Uniaxial compressive strain εc1, ‰	-2
Uniaxial ultimate compressive stress fck, MPa	-23
Uniaxial ultimate compressive strain εcu2, ‰	-3.5
Density r, kg/m3	2500
Poisson's ratio ν	0.2

Table 2: Properties of the concrete used in the numerical model of beam.

The steel section and the concrete slab were modelled using 8-node 3D-solid finite elements. Rebar elements were used to model the reinforcing bars. The sheets were modelled with 8-node shell elements, and the nails with 2-node beam elements. Pneumatic actuators and supports were simulated using 8-node 3D-solid elements.

The interactions between the components in the finite element models were as follows:

- Connection of the sheet with the concrete slab by means of common nodes;
- Connection of the concrete slab with reinforcement bars using rebar elements;
- Connection of the I-beam with the slab as well as nails and the slab using common nail and I-beam nodes;
- "Mesh gluening" to connect the supports with the I-beam and the actuators with the slab.

4 Sensitivity analysis of numerical model

The numerical model used to parameterize the steel-concrete composite beam was developed based on the results of the sensitivity assessment. Four variants of numerical models of the beam were built, differing in the number of nodes in the finite elements of the steel beam, concrete slab and corrugated sheet, which is presented in Table 3. The adopted numerical model mesh is shown in Figure 4.

The deflection - external load diagrams for each of the analysed variants are shown in Figure 5. Table 3 shows the deflection values at two points corresponding to the external load of 56 and 160 kN. In addition, percentage references of deflections are presented. The deflection corresponding to 100% was assumed for model 1.

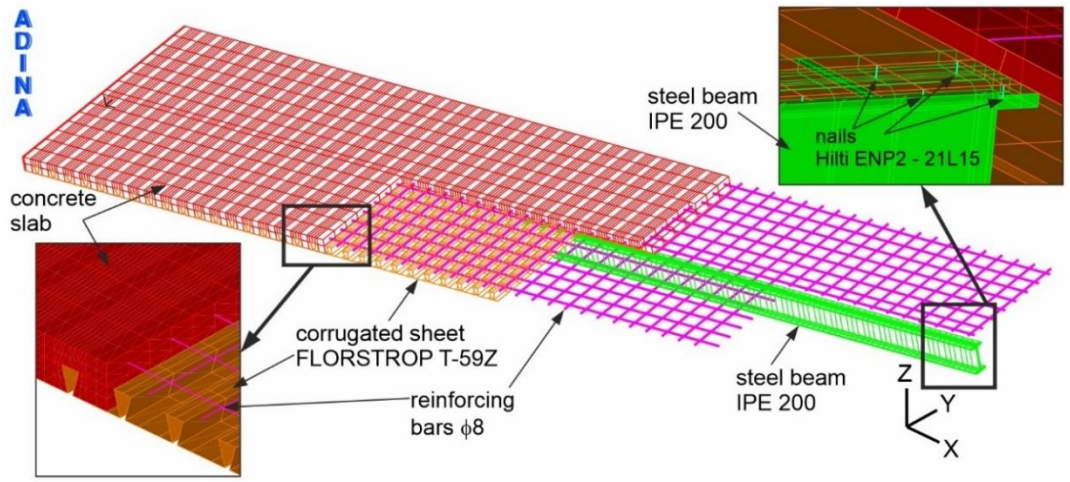

Figure 4: Mesh of composite beam numerical model.

Element group	Number of nodes			
	Variant 1	Variant 2	Variant 3	Variant 4
Steel beam (3D-solid elements)	27	27	20	20
Concrete slab (3D-solid elements)	27	27	20	20
Steel sheet (shell elements)	8	16	8	16
Nails (beam elements)	2	2	2	2
Actuators and supports (3D-solid elements)	8	8	8	8
Deflection under load 56 kN, mm	24.15	24.46	24.03	24.27
Deflection under load 56 kN, %	100%	101%	100%	101%
Deflection under load 160 kN, mm	91.09	99.88	89.21	97.76
Deflection under load 160 kN, %	100%	110%	98%	107%

Table 3: Sensitivity analysis due to number of nodes in finite elements.

As can be seen in Figure 5, the numerical model of the composite beam in a small alloy is sensitive to the number of nodes of finite elements. The deflection values at the point corresponding to the load of 56 kN are similar and amount to 100 – 101% compared to the reference model. The deflection values at the point corresponding to the load of 160 kN are in the range of 89.21 – 99.88, which is 98 – 110% compared to the deflection of the reference model. The applied finite elements allowed for the convergence of the beam stiffness in the elastic range with the experimental results. At the same time, the convergence of the results from the simulation and the experiment in the curvilinear range was observed.

It was found that the 8-node shell elements reflecting the corrugated sheet provide sufficient calculation accuracy, and at the same time require less computational resources in relation to the 16-node finite elements. It was decided to use 27-node 3D-solid finite elements for the I-beam and concrete slab. They require more computing power than 20-node elements, but allow for more accurate analysis of concrete elements. Therefore, variant 1 was selected for further analysis.

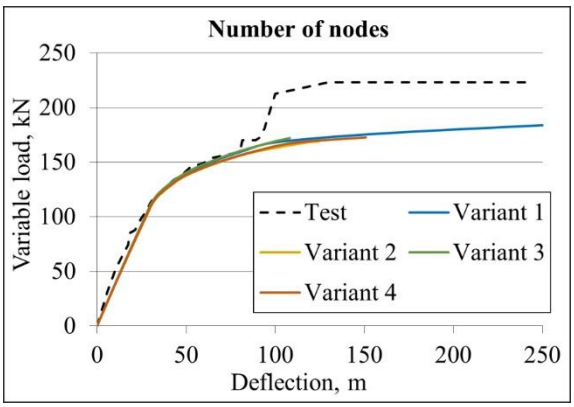

Figure 5: Deflection – variable load graph for assessment of sensitivity analysis due to number of nodes.

The second criterion used to evaluate the sensitivity was the mesh size in the IPE beam web. The web was discretized with two different finite element meshes characterized by 1 and 3 elements at the height of the web, as shown in Figure 6. Changing the mesh size affected the number of finite elements (Table 4). The sensitivity analysis was carried out only for variant no. 1, built of 27-node 3D-solid finite elements for the I-section and concrete slab, and 8-node finite elements of the shell type for the corrugated sheet. In this case, variant no. 1A was distinguished corresponding to variant no. 1 from the first criterion of the sensitivity analysis (Figure 6) and variant 1B.

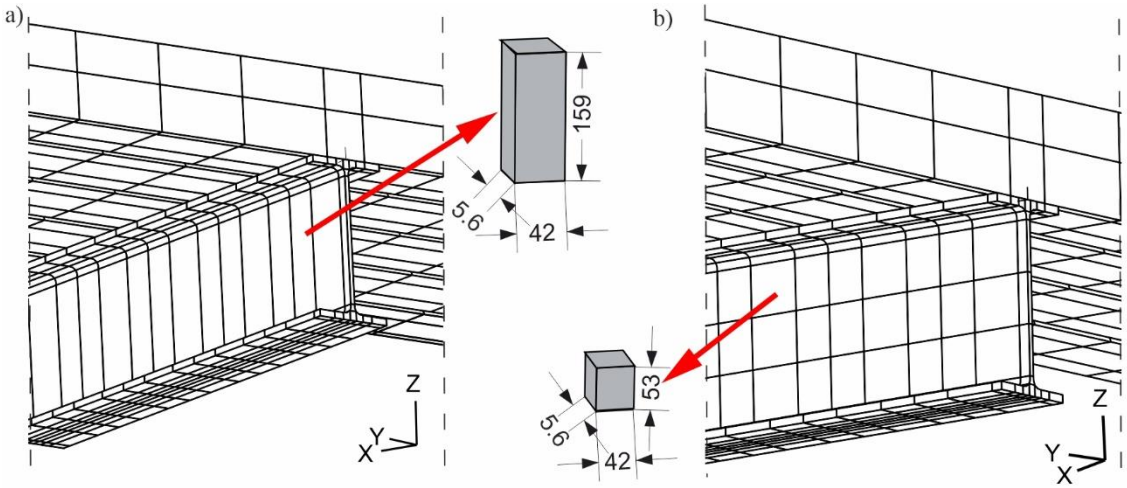

Figure 6: Mesh variants included in sensitivity analysis: a) variant 1A b) variant 1B, mm.

Element group	Number of finite elements	
	Variant 1, 2, 3, 4 (due to the number of nodes) Variant A (due to the number of finite elements)	Variant B due to the number of finite elements)
No 1 (3D-solid) representing a steel beam	2 754	8 262
No 2 (3D-solid) representing a concrete slab	6 450	6 450
No 3 (rebar) representing reinforcing bars	4 824	4 824
No 4 (beam) representing nails	912	912
No 5 (shell) representing sheet metal	5 610	5 610
No 6 (3D-solid) representing actuators	16	16
No 7 (3D-solid) representing supports	4	4
Sum	20 570	26 078

Table 4: Number of finite elements used for sensitivity analysis.

Deflection-external load diagrams for both variants are shown in Figure 7. The curves for variants 1A and 1B coincide, which proves that the numerical model of the composite beam is not sensitive to the number of finite elements at the height of the steel beam web.

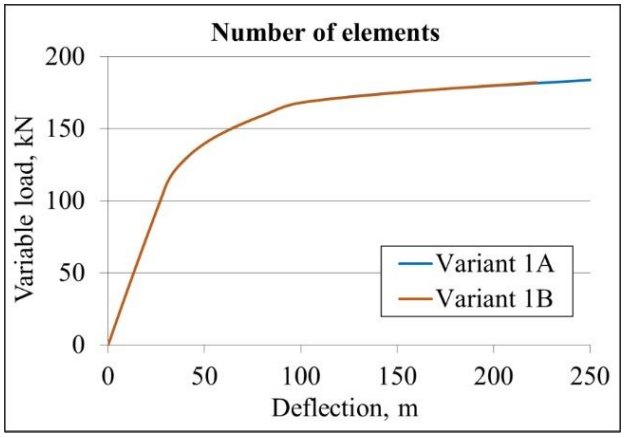

Figure 7: Deflection – variable load graph for assessment of sensitivity analysis due to number of finite elements represented web.

5 Results

Comparison of the deflection-load diagrams for the composite beam obtained experimentally (orange) and numerically (blue) is shown in Figure 8. It is easy to notice the convergence of the curves in the initial phase of the graph, i.e. in the elastic range. This proves that the stiffness of the composite beam analysed experimentally is similar to its numerical equivalent. However, the load at which the beam changes from elastic to plastic, determined on the basis of the results of experimental tests, is 116.9 kN. However, the force determined on the basis of numerical simulation is about 10% lower, because it is equal to 104 kN. The difference is due to the tolerance of beam manufacturing, which was 1 mm for steel parts and 10 mm for concrete parts.

The maximum load transferred by the beam during the experiment is 223 kN, and numerically determined is 184 kN, which is 21% less. The adopted material models, especially the concrete model, contribute to the difference to the disadvantage of the simulation, so the calculations ended after the occurrence of cracks marked with the number 4, i.e. after cracked of the concrete on the upper surface of the slab in the place of the actuators' pressure. It should be noted that even under the action of a load of 104 kN in the concrete slab (Figure 9), the tensile stresses at the contact point of the slab with the actuators are 6.58 MPa and exceed the ultimate tensile strength of the concrete, which is equal to 2.2 MPa. It is only a local stress concentration resulting from the action of a concentrated load. With a load of 104 kN in the rest of the slab, the compressive and tensile stresses do not exceed the ultimate strength of the concrete.

In the last step of the calculations (Figure 10), representing a load of 184 kN, a similar dependence of the local concentration of compressive and tensile stresses at the point of action of the concentrated load can be observed. However, the values of these stresses take on much larger values. In order to reduce the crushing effect of concrete at the pressure point of the actuators, in subsequent research works it is suggested to use a flat plate between the actuators and the slab. It is worth emphasizing that both during the experiment and in numerical calculations, the cause of the beam failure were scratches in the slab.

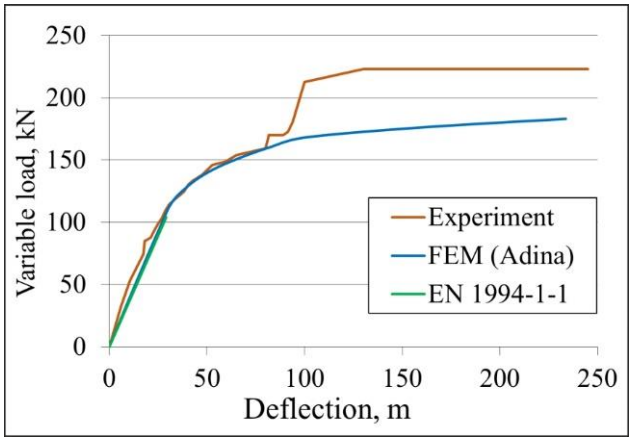

Figure 8: Deflection-load graph comparing experimental and numerical results.

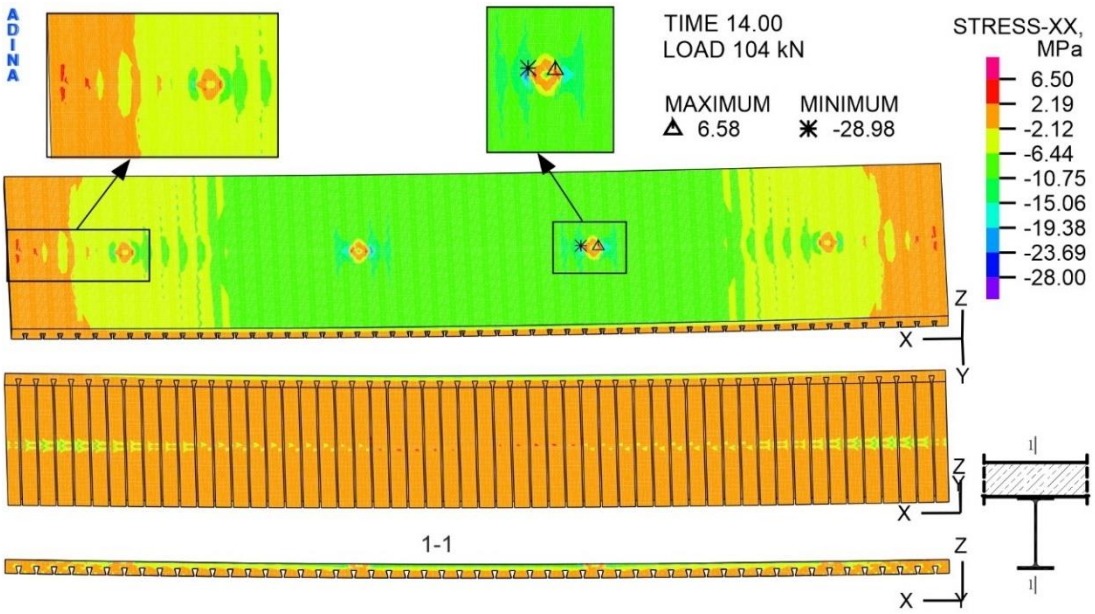

Figure 9: Distribution of stress with respect to X-axis in concrete slab, load of 104 kN, MPa.

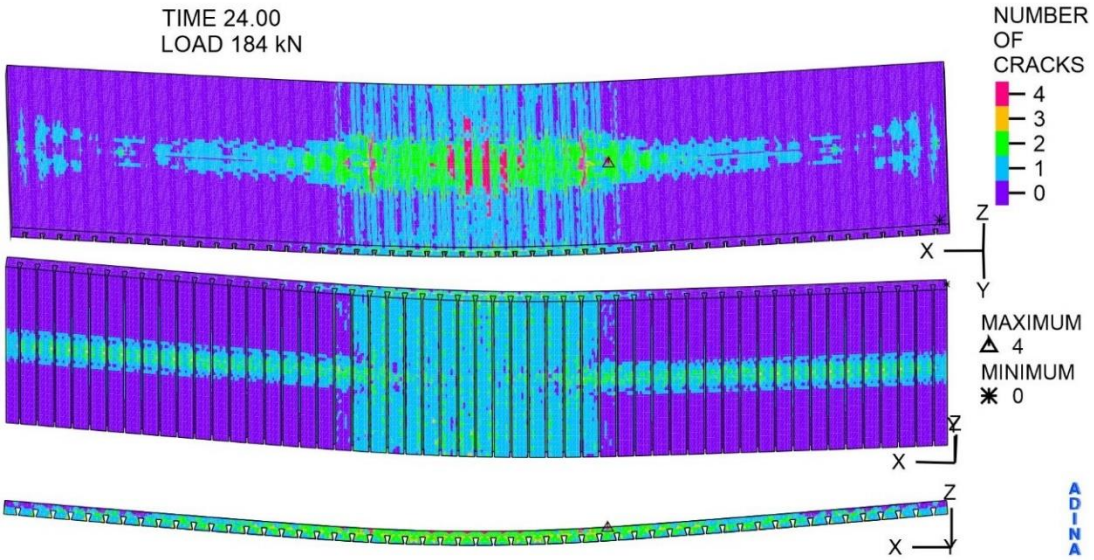

Figure 10: Cracks in concrete, load of 184 kN, -.

The distribution of directional stresses with respect to X-axis in the IPE I-beam were presented in Figure 11 and 12. Under a load of 104 kN, the middle part of the IPE is in tension. In the support zones of the I-beam, the web is in compression and both flanges are in tension. At the same time, in the support area, the upper flange in the area where the nails enter is compressed. The extreme of the I-beam tensile stress occurs in the middle of the bottom flange span and is 323.1 MPa. This value is slightly lower than the determined yield strength of the I-beam material, which is 339 MPa. The compressive stress extreme of 62.5 MPa is located in the upper flange, in the support zone.

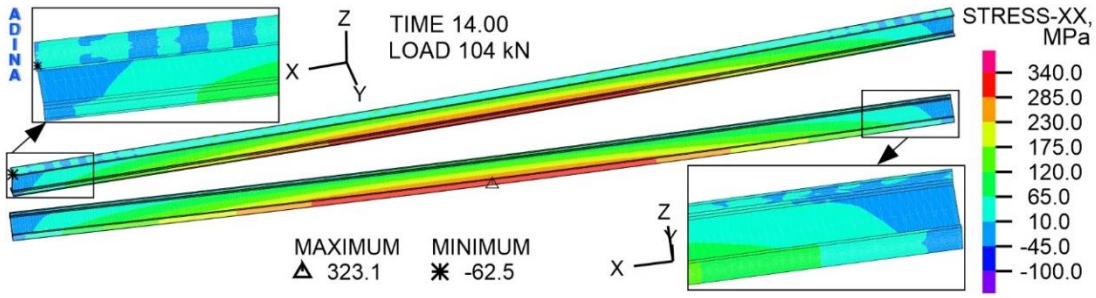

Figure 11: Distribution of stress with respect to X-axis in steel component of IPE 200, load of 104 kN, MPa.

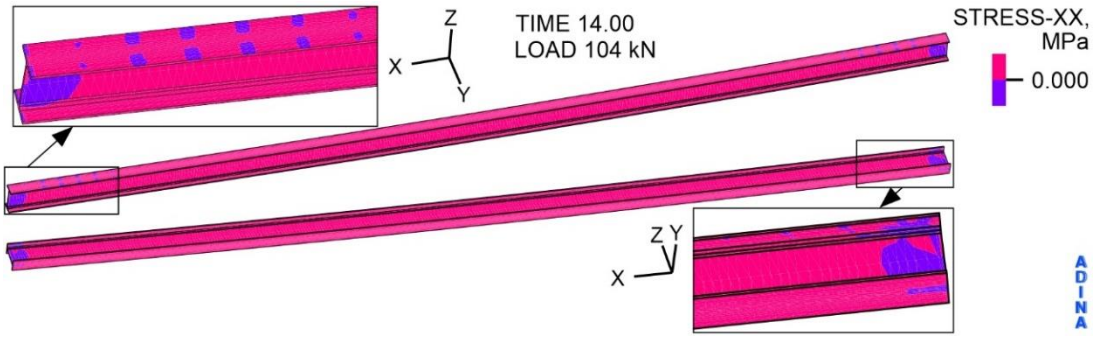

Figure 12: Distribution of stress with respect to X-axis in steel component of IPE 200, load of 104 kN, MPa.

The analysed composite beam behaves elastically up to a load of 116.9 kN, which corresponds to a design floor load of 8.6 kN/m^2. Assuming a partial factor of 1.5 according to Eurocode 4 [26], a floor beam can carry a characteristic load of 5.7 kN/m^2. Therefore, the proposed solution of fasteners for composite structures met the assumed expectations

6 Conclusions and Contributions

1. The analysed composite beam behaves elastically up to a load of 116.9 kN, which corresponds to a design floor load of 8.6 kN/m^2. According to the requirements of Eurocode 4, a floor beam can carry a characteristic load of 5.7 kN/m^2.
2. Based on the results of experimental tests, it was found that the beam connectors showed sufficient load-bearing capacity, and the concrete slab was the weakest component of the composite beam. The beam was damaged as a result of cracking in the slab and, as a consequence, local detachments of the corrugated sheet from the concrete slab.
3. The carried out numerical calculations showed that the mechanism of concrete slab failure is related to the formation of a plastic hinge in the middle of the span of the steel beam and plastic deformations occurring in the corrugated sheet in the middle of its width. Plastic deformations of the upper and lower folds of the sheet contributed to delamination between the sheet and the concrete slab.
4. Based on the experimental tests and numerical calculations, it was found that the proposed solution of fasteners made of corrugated sheet and shot nails can be used as the fastener for steel-concrete composite structures applied in lightweight ceilings of small utility public buildings.
5. The developed numerical model of the composite beam allows the optimalization of the beam cross-section and optimalization of the connector depending on the assumed boundary conditions, the manner and size of the acting load.

References

[1] A. Feyissa, G. Kenea, "Performance of Shear Connector in Composite Slab and Steel Beam with Reentrant and Open Trough Profiled Steel Sheeting", Advances in Civil Engineering, 2022, 1–14, 2022. doi: 10.1155/2022/5010501

[2] S. Gao, Y. Xu, S. Zhang, A. Derlatka, "Performance of square concrete-filled steel tubular columns under repeated lateral impact", Eng. Struct., 280, 115719, 2023. doi: 10.1016/j.engstruct.2023.115719

[3] P. Lacki, A. Derlatka, P. Kasza, S. Gao, "Numerical study of steel–concrete composite beam with composite dowels connectors", Comput. Struct., 255, 106618, 2021. doi: 10.1016/j.compstruc.2021.106618

[4] M. Abramowicz, S. Berczyński, T. Wróblewski, "Modelling and parameter identification of steel–concrete composite beams in 3D rigid finite element method", Arch. Civ. Mech. Eng., 20, 4, 2020. doi: 10.1007/s43452-020-00100-7

[5] M. Chybiński, Ł. Polus, "Structural Behaviour of Aluminium–Timber Composite Beams with Partial Shear Connections", Applied Sciences, 13, 3, 1603, 2023. doi: 10.3390/app13031603

[6] M. Chybiński, Ł. Polus, W. Szwabiński, P. Niewiem, "Fe analysis of steel-timber composite beams" in "Proceedings of the 15th Conference on Computational Technologies in Engineering", Jora Wielka, Poland, 20061, 2019.

[7] P. Szewczyk, M. Szumigała, "Optimal Design of Steel-Concrete Composite Beams Strengthened under Load", Materials, 14, 16, 2021. doi: 10.3390/ma14164715

[8] A. Derlatka, P. Lacki, P. Kania, S. Gao, "Study of Innovative Connector for Steel–Concrete Composite Structures", Applied Sciences, 14, 7, 3003, 2024. doi: 10.3390/app14073003

[9] Eurocode 4: Design of composite steel and concrete structures - Part 1-1: General rules and rules for buildings, EN 1994-1-1, European Committee For Standardization (CEN), 2008.

[10] ADINA System Online Manuals. ADINA R&D, Inc., 2020.

[11] K.-J. Bathe, J. Walczak, A. Welch, N. Mistry, "Nonlinear analysis of concrete structures", Comput. Struct., 32, 3-4, 563–590, 1989. doi: 10.1016/0045-7949(89)90347-7

[12] Design of concrete structures - Part 1-1: General rules and rules for buildings, EN 1992-1-1, European Committee For Standardization (CEN), 2008.

[13] Eurocode 3: Design of steel structures - Part 1-1: General rules and rules for buildings, EN 1993-1-1, European Committee For Standardization (CEN), 2006.